Catal Lett (2007) 119:353–360
DOI 10.1007/s10562-007-9244-0

Effect of the Ratio of Precipitated SiO_2 to Binder SiO_2 on Iron-based Catalysts for Fischer–Tropsch Synthesis

Wenjuan Hou · Baoshan Wu · Xia An · Tingzhen Li · Zhichao Tao · Hongyan Zheng · Hongwei Xiang · Yongwang Li

Received: 19 June 2007 / Accepted: 14 August 2007 / Published online: 6 September 2007

Abstract The effects of the ratio of precipitated SiO_2 to binder SiO_2 (Si(P)/Si(B)) on the reduction, carburization and catalytic behavior of precipitated Fe–Cu–K–SiO_2 catalysts for Fischer–Tropsch synthesis (FTS) were investigated by N_2 physisorption, temperature-programmed reduction/desorption (TPR/TPD) and Mössbauer effect spectroscopy (MES). FTS performances of the catalysts were tested in a continuous stirred tank reactor (CSTR). It is found that the increase of Si(P)/Si(B) ratio (Si(P)/Si(B) = 0/25 ∼ 15/10) decreases the crystallite size of the catalysts, improves the surface basicity, enhances the reduction and carburization of the catalysts, and increases the activity of the catalyst. However, when Si(P)/Si(B) ratio is further increased (Si(P)/Si(B) = 25/0), the catalyst exhibits a restrained reduction and carburization behavior, which may be attributed to the stronger metal–support interaction. Based on the present work, a catalyst with a suitable ratio of Si(P)/Si(B), for example Si(15)/Si(10) displays an optimal FTS performances.

Keywords Fischer–Tropsch synthesis · Precipitated SiO_2 · Iron catalyst · Mössbauer effect spectroscopy

W. Hou · B. Wu · X. An · T. Li · Z. Tao · H. Zheng · H. Xiang · Y. Li (✉)
State Key Laboratory of Coal Conversion, Institute of Coal Chemistry, Chinese Academy of Sciences, Taiyuan 030001, P.R. China
e-mail: ywl@sxicc.ac.cn

W. Hou · X. An · T. Li · Z. Tao · H. Zheng
Graduate University of Chinese Academy of Sciences, Beijing 100039, P.R. China

1 Introduction

Fischer–Tropsch (FT) synthesis is an attractive route to produce environmentally friendly fuels and other chemicals from syngas derived from coal, natural gas and biomass [1, 2]. Iron based catalysts are preferred for FTS due to their low cost, higher water gas shift (WGS) reactivity, which helps to make up the deficit of H_2 in the syngas from coal gasification [3–5]. Attrition problem of an iron catalyst has become a concern, especially when it is used in a slurry bubble column reactor (SBCR) [5–7]. Structural promoters (SiO_2, Al_2O_3, and other support materials) are generally used in iron catalyst to improve attrition resistance and stability [6, 8]. Nevertheless, catalysts containing a binder or support usually suffer from lowered FTS activity [9, 10]. Many studies attributed the reactivity loss to strong metal–support interaction [11–14]. Recently, Wan et al. [11] and Zhang et al. [12] investigated the FTS performances of simple Fe/Al_2O_3 and Fe/SiO_2 systems, respectively. The results proved that the existence of metal–support interaction lowered the FTS activity of a catalyst. Dlamini et al. [13] investigated the effect of the incorporation step of SiO_2 on precipitated Fe/Cu/K/SiO_2 catalyst. They found that SiO_2 added during precipitation (precipitated SiO_2) induced a stronger metal–support interaction than that added after precipitation (binder SiO_2), so the former showed lower FTS activity. Yang et al. [14] also investigated the impacts of incorporation step of SiO_2 on the reduction and FTS performances over the precipitated Fe–Mn–K–SiO_2 catalyst. The results showed that the catalyst with precipitated SiO_2 (SiO_2 was incorporated during precipitation) exhibited a stronger interaction between Fe and SiO_2 than that with binder SiO_2 (SiO_2 was incorporated after precipitation), but the former displayed higher FTS activity. The result is inconsistent with that obtained by Dlamini.

Most investigations were focused on the effects of the addition of SiO_2 on the catalytic behaviors. However, few of them could describe the differences between precipitated SiO_2 and binder SiO_2. And some conclusions are in controversy. There is a lack of detailed information on how the SiO_2 incorporation (delete) affects the extent of metal–support interaction.

In this paper, based on the industrial catalyst composition 100Fe/5Cu/4K/25SiO_2, a series of Fe/Cu/K/SiO_2(P)/SiO_2(B) catalysts with different Si(P)/Si(B) ratio were prepared by using co-precipitated method. Several effective characterization techniques, including H_2-TPR, CO_2-TPD, and MES were used to investigate the effects of the ratio of Si(P)/Si(B) on reduction and carburization of the catalysts. Slurry phase FTS reactions of the catalysts were monitored. The work aims at providing some useful information on the different extents of Fe–SiO_2 and K–SiO_2 interaction aroused by the different ratio of Si(P)/Si(B) in the Fe/Cu/K/SiO_2(P)/SiO_2(B) catalysts, which affect the FTS performance greatly.

2 Experimental

2.1 Catalyst Preparation

A series of Fe/Cu/K/SiO_2 catalyst samples in the present work were prepared using the combination of co-precipitation and spray-drying method. All the catalysts were prepared with the same ratio of iron, copper, potassium and silica (100Fe/5Cu/4K/25SiO_2) as the benchmark, but with different levels of binder SiO_2 and precipitated SiO_2. In brief, a solution containing $Fe(NO_3)_3 \cdot 9H_2O$ (99.9%+), $Cu(NO_3)_2 \cdot 3H_2O$ (99.9%+) and (when added) SiO_2 sol solution (as precipitated SiO_2) at the desired Fe/Cu/SiO_2 (p) ratios was precipitated continuously using a sodium carbonate solution (99.9%+) as a precipitating agent at 80 ± 1 °C and pH = 8.0 ± 1. The precipitates was then filtered and washed with deionized water. The filtered cake was re-slurried in deionized water, and then added with appropriate amount of SiO_2 sol solution (as binder SiO_2) and K_2CO_3 solution. The mixture was then re-slurried and spray-dried. The obtained catalyst precursors were calcined at 400 °C for 5 h in a muffle furnace. The final obtained fresh catalysts exhibit good spherical particles with a size range of 20–80 μm.

The composition of the five catalysts are 100Fe/5Cu/4.2K/$x$$SiO_2$(P)/$y$$SiO_2$(B) ($x$ = 0, 5, 15, 25, y = 25 − x) in mass ratio, which are labeled as Si0/25, Si5/20, Si15/10, Si25/0, respectively. Detailed descriptions of the catalysts are presented in Table 1.

2.2 Catalyst Characterization

BET surface area, pore volume and the pore size of the catalysts were determined via a Micromeritics ASAP 2500, using N_2 physisorption at its normal boiling point (77 K). The samples were degassed under vacuum at 180 °C for 6 h before measurement.

Temperature-programmed reduction (TPR) in H_2 atmosphere was performed to investigate the reduction behavior of the catalysts in a conventional atmospheric quartz flow reactor (5 mm i.d.) using a mixture gas of 5% H_2/95% Ar (on mole basis). The flow rate of the reduction gas was 50 mL/min in the standard state and the TPR profiles were recorded by using the thermal conductivity detector (TCD) to monitor the variation of H_2 concentration. An on-line dried trap (in the H_2-TPR) located between the reactor and TCD detector was used remove continuously water produced during reduction. Typically, 40 mg catalyst was loaded and reduced by raising temperature from 20 °C to 817 °C at 10 °C/min.

CO_2-TPD was performed in the same system as in TPR with helium as the carrier gas. CO_2 desorption was measured by TCD. Typically, 200 mg sample was loaded in the reactor. First, the catalyst was heated in the carrier gas (50 NmL/min) from room temperature to 400 °C, and then held at 400 °C until the base line leveled off and then cooling down to 50 °C for TPD. The flow was switched to CO_2 (purity: 99.95%) at 50 °C for 30 min, and then followed by purging with helium for 1 h to remove weakly adsorbed species. After the step, catalyst sample was then heated to 430 °C at 6 °C/min in a flow of He and the TPD spectra was recorded.

The Mössbauer spectroscopy of catalysts were recorded at room temperature using a CANBERRA Series 40 MCA (USA) constant-acceleration Mössbauer spectrometer and a 25-m Ci ^{57}Co in Pd as γ-ray source. The spectrometer was operated in the symmetric constant acceleration mode. The spectra were collected over 512 channels in the mirror-image format. Data analysis was performed using nonlinear least squares fitting routine that models the spectra as a combination of singlets, quadruple doublets, and magnetic sextets based on a Lorentzian line shape profile. The spectral components were identified based on their isomer shift (IS), quadruple splitting (QS) and magnetic hyperfine field (Hhf). All isomer shift values were reported with respect to metallic iron (α-Fe). Magnetic hyperfine fields were calibrated with the 330 KOe field of α-Fe at ambient temperature.

2.3 Fischer–Tropsch Synthesis

The FTS performance of catalysts was tested in a 1 dm^3 continuously stirred tank reactor (CSTR) loaded with

Table 1 The composition and textural properties of the calcined catalysts

Catalyst	Catalyst composition (parts by weight)	BET surface area (m^2/g)	Pore volume (cm^3/g)	Average pore size (nm)
Si0/25	100Fe/5Cu/4K/0Si(P)/25Si(B)	171	0.21	4.71
Si5/20	100Fe/5Cu/4K/5Si(P)/20Si(B)	197	0.24	4.82
Si15/10	100Fe/5Cu/4K/10Si(P)/20Si(B)	235	0.37	6.37
Si25/0	100Fe/5Cu/4K/25Si(P)/0Si(B)	241	0.31	5.11

20.0 g catalyst sample and 330 g liquid paraffin. A detailed description about the reactor and the product system was given elsewhere [14, 15].

The catalyst was reduced in situ in syngas (H_2/CO = 1.2) at 280 °C, 0.1 MPa and 1.0 NL/g-cat/h for 24 h. After reduction, steady-state reaction conditions were set as 250 °C, 1.5 MPa, H_2/CO = 0.67 and 2.0 NL/g-cat/h.

3 Result and Discussion

3.1 Textural Properties of the Calcined Catalysts

The BET surface area, pore volumes and average pore diameters of the calcined catalysts are given in Table 1. It can be seen that the surface area increases with increasing Si(P)/Si(B) ratio obviously, whereas the average pore diameter and the pore volume change slightly. The fact that the precipitated SiO_2 could result in catalysts with higher surface area has also been found by many researchers [5, 13, 14]. This can be attributed to that the precipitated SiO_2 could provide a more dispersed rigid matrix, which helps to prevent the catalyst from fast pore collapse and stabilizes the small iron oxide crystallites from sintering more effectively than the binder SiO_2 [9, 16]. In other word, the precipitated SiO_2 is in favor of the high dispersion of α-Fe_2O_3. Consequently, smaller crystallite size and the porous structure was formed, and larger surface area were observed with increasing Si(P)/Si(B) ratio. Mössbauer spectroscopy of the calcined catalysts discussed later gives the similar result.

3.2 Reduction and Carburization Behaviors

H_2-TPR was used to investigate the effect of Si(P)/Si(B) ratio on the reduction behavior of the catalysts. The profiles of H_2-TPR and quantitative results are presented in Fig. 1 and Table 2, respectively. As shown in Fig. 1, two-stage reduction process of α-Fe_2O_3 occurs. It has been accepted that the first stage (250–350 °C) corresponds to the reduction of $CuO \rightarrow Cu$ and α-$Fe_2O_3 \rightarrow Fe_3O_4$, whereas the second stage (350–700 °C) corresponds to the reduction of Fe_3O_4 to metallic Fe [9, 17]. However, comparing the experimental peak areas with their corresponding theoretical ones listed in Table 2, it can be seen that the reduction of α-Fe_2O_3 during the first stage possibly proceed other than Fe_3O_4, and the reduction during the second stage is incomplete [18].

In detail, the amounts of H_2 consumption for reduction peaks at lower temperature (270–350 °C) 0.30–0.38 mol H_2/mol M(Fe + Cu) for all the catalysts are larger than the theoretical value corresponding to the transformation of $CuO \rightarrow Cu$ and $Fe_2O_3 \rightarrow Fe_3O_4$ [0.2 mol H_2/mol M(Fe + Cu)], but it is lower than those of $CuO \rightarrow Cu$ and $Fe_2O_3 \rightarrow FeO$ [0.51 mol H_2/mol M(Fe + Cu)]. It is postulated that the first stage can be ascribed to the reduction of $CuO \rightarrow Cu$, α-$Fe_2O_3 \rightarrow Fe_3O_4$ and part of $Fe_3O_4 \rightarrow FeO$. The existence of FeO at the first reduction stage in TPR for the catalyst incorporated with SiO_2 has been reported by many reports [12, 14, 18, 19]. It is reasonable to suppose that the FeO phase is stabilized by the support. From Fig. 1 and Table 2, it can be seen that the amount of H_2 consumed at the first stage increases from 0.30 to 0.38 mol H_2/mol M with increasing Si(P)/Si(B) ratio. The result demonstrates that the increase of Si(P)/Si(B) ratio improves the reduction at the first stage, characterized by the fact that more Fe_3O_4 was reduced to FeO.

The second reduction stage at high temperature (400–700 °C) can be ascribed to the reduction of $Fe_3O_4 \rightarrow Fe$ and $FeO \rightarrow Fe$ [9, 15]. It should be noted that the second

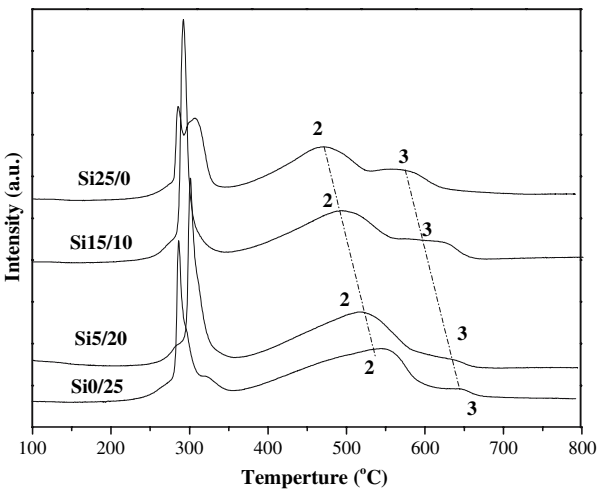

Fig. 1 H_2-TPR profiles of the catalysts

Table 2 Quantitative results of H_2-TPR for catalysts

Catalyst samples	Peak maximum (°C)	Component hydrogen consumption	
		mol H_2/mol M[a]	mol H_2/mol Fe
Si0/25	286	0.0897	
	294	0.216	
	511		1.13
	649		0.00001
Si5/20	303	0.31	
	506		1.09
	622		0.003
Si15/10	292	0.33	
	486		1.06
	610		0.039
Si25/0	286	0.074	
	306	0.297	
	467		0.84
	571		0.16

[a] M = Fe + Cu

stage can be further separated into two peaks. The peak 2 at 460–480 °C can be ascribed to the partly reduction of Fe_3O_4 to Fe or FeO, and the peak 3 at 527–650 °C possibly represent the reduction of FeO to Fe. Moreover, the area of peak 2 decreases whereas the area of peak 3 increases with increasing Si(P)/Si(B) ratio. This result may suggest that more precipitated SiO_2 enhances Fe–SiO_2 interaction by stabilizes the wustite phase (FeO) [12], resulting in the difficulty of further reduction. However, it is also found that the reduction temperatures of peak 2 and 3 both shift to lower temperature with increasing Si(P)/Si(B) ratio, indicating that the increase of Si(P)/Si(B) ratio enhances the reduction at the second stage to some extent. The probable reason is that the catalyst with higher Si(P)/Si(B) ratio may have a better dispersion of iron oxide, suppressing the growth of crystallite at the high temperature (460–650 °C), which make the reduction peak shift to low temperature. Mössbauer spectroscopy of the calcined catalysts discussed later gives the estimation of crystallite size of the catalysts. The combined effects will determine the reduction of the catalyst at the second stage.

Yang [14] and Dlamini et al. [13] have proposed that the catalyst incorporated with precipitated SiO_2 is more difficult to be reduced than those incorporated with binder SiO_2 due to the strong SiO_2–metal interaction. Moreover, the Fe–SiO_2 interaction can stabilize Fe_3O_4 or FeO and restrain them to proceed further reduction [12, 19]. It is reasonable to deduce that the increase of Si(P)/Si(B) ratio may restrain the reduction of Fe_2O_3, due to the enhanced SiO_2–metal interaction. However, another effect should be taken into consideration. The increase of Si(P)/Si(B) ratio brings to larger BET surface area, resulting highly dispersion of Fe_2O_3 and CuO phases [15], therefore facilitating the reduction. In the present study, both the metal–support interaction and the iron phase dispersion affect the reduction behavior of the catalyst [20]. For this reason, it can be seen in Table 4 that the reduction degree of iron oxide increases with Si(P)/Si(B) ratio, except for Si25/Si0, which exhibits the strongest Fe–SiO_2 interaction, but it is the most porous catalyst (see Table 3), which implying a good dispersion of iron phase.

The CO_2-TPD profiles of all catalysts are shown in Fig. 2. The CO_2 uptakes can be used to indicate the intensity of the surface basicity. In general, there are three desorption peaks in the TPD profiles. One at the lower temperatures (50–135 °C) corresponds to weak CO_2 adsorption, while the other two at higher temperatures (135–208 °C, 208–400 °C) are ascribed to the adsorption of CO_2 that interacts moderately with the surface basic site. It is found that there is little change in temperature for two peaks (peak 1 and peak 2), whereas the areas of the two peaks increase, and the third peak shifts to higher temperature with increasing Si(P)/Si(B) ratio. The result indicates that the surface bacisity increases with increasing Si(P)/Si(B) ratio. As mentioned above, the increase of Si(P)/Si(B) ratio improves the dispersion of the metal (Fe, K), more surface basic sites can expose to the surface of the

Table 3 Mössbauer parameters of the calcined catalysts

Catalyst	Phases	MES parameter				
		IS (mm/s)	QS (mm/s)	Hhf (kOe)	Area (%)	d_P (nm)
Si0/25	α-Fe_2O_3	0.36	–0.21	485	35.1	>6.57
	Fe^{3+} (spm in bulk)	0.24	0.66		49.2	
	Fe^{3+} (spm in surface)	0.24	1.20		15.7	
Si5/20	Fe^{3+} (spm in bulk)	0.24	0.64		67.6	1.9
	Fe^{3+} (spm in surface)	0.22	1.12		32.4	
Si15/10	Fe^{3+} (spm in bulk)	0.35	0.60		61.8	1.5
	Fe^{3+} (spm in surface)	0.33	1.06		38.2	
Si25/0	Fe^{3+} (spm in bulk)	0.34	0.65		60.5	1.4
	Fe^{3+} (spm in surface)	0.33	1.16		39.5	

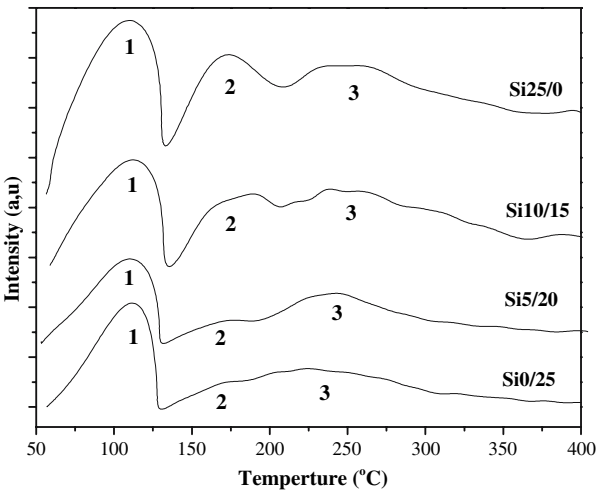

Fig. 2 CO_2-TPD of the catalysts

catalyst, resulting in the increase of the surface basicity. At the same time, the enhancement of Fe–SiO_2 interaction with increase of Si(P)/Si(B) ratio weakens the SiO_2–K relation to some extent, increasing also basic function of K.

The MES parameters and the iron-phase composition for the catalysts at the different stage are listed in Tables 3–5, respectively, as determined by fitting the Mössbauer spectra. As shown in Table 3, the sextet can be assigned to the paramagnetic α-Fe_2O_3 with the crystallite diameters larger than 13.5 nm and the doublet is typical for the superparamagnetic (spm) Fe^{3+} ions on the non-cubic sites with the crystallite diameters smaller than 13.5 nm [21, 22]. More precisely, the spectrum was analyzed by two doublets with equal isomeric shift (IS) values, but different quadruple splitting (QS) values. These different QS values can be attributed to the Fe^{3+} ions located in the bulk of the crystallites (low QS values) and the ones situated on the surface of the particles (high QS values). An estimation about the average crystallite was obtained from: $d_P = 0.9/D$, where d_P is the average crystallite diameter in nm and D is the ratio of the spectral area corresponding to atoms located on the "surface" to those located in the "bulk" of the crystallites [13, 14]. On the basis of the above analysis, as shown in Table 3, the estimating average crystallite diameter from Mössbauer spectroscopy decreases with the increase Si(P)/Si(B) ratio. And one can find that substituting small amount of binder SiO_2 by precipitated SiO_2 (Si(P)/Si(B) = 5/20) results in a significant decrease in average crystallite size. The d_P value changes from >6.59 for the catalyst with no precipitated SiO_2 to 1.9 for the catalyst with Si(P)/Si(B) = 5/20.

As shown in Table 4, the reduced catalysts are mainly composed of Fe^{2+}, Fe^{3+} species in superparamagnetic state and iron carbides. It is found that the content of iron carbides (χ-Fe_5C_2 + ε'-$Fe_{2.2}C$) increase following the order of Si0/25 (45.2%), Si5/20 (49.4%), Si15/10 (62.1%), then decreases for Si25/0 (56.9%), indicating that the carburization of the catalysts is promoted with increasing Si(P)/Si(B) ratio but is restrained when the catalyst was totally cooperated with precipitated SiO_2 (Si25/0). Moreover, the degree of reduction shows the similar trend. The result is in agreement with that of H_2-TPR and CO_2-TPD. The probable reason is that the increase of Si(P)/Si(B) ratio enhances the dispersion of active phase and increases the surface basicity, which improves the reduction and carburization of the catalyst. On the other hand, the metal–support interaction is strengthened with increasing Si(P)/Si(B) ratio, which stabilizes more small iron crystalline and restrains the reduction and carburization of the catalysts to some extent [9, 14, 23].

As shown in Table 5, after a longer reaction, carbide contents decrease and amounts of spm Fe^{2+} and spm Fe^{3+}species increase for all catalysts. It indicates that some of the carbides are reoxidized by water and undergo further phase transformation under the FT reaction condition [24].

3.3 FTS Performance

FTS performance of series of catalysts was tested under conditions of 250 °C, 1.5 MPa, H_2/CO = 0.67 and 2.0 NL/g-cat/h which are typical reactions for an industrial practice over a precipitated iron catalyst. The run time on stream is 480–520 h.

3.3.1 Activity and Reaction Stability

The FTS performances of the catalysts are presented in Fig. 3 and Table 6. It is found that the catalyst activity increases with increasing Si(P)/Si(B) ratio, then passes through a maximum for Si15/10, and then declines for Si25/0 with only precipitated SiO_2. The group catalysts are stable with time on stream (TOS). It should be noted that all the catalysts with precipitated SiO_2 exhibit obvious FTS reactivity than that with only binder SiO_2. It is known that the catalyst activity is correlated with the formation of active phases, and the number of the active sites [25] or the density of the active sites in near surface layers [26, 27]. Iron carbides have been supposed to be the most likely the FTS active phases for an iron based catalyst [15, 19, 26, 28, 29]. Therefore the content of iron carbides in bulk phase can be used to monitor the formation of FTS active sites indirectly. In general, for most of catalysts, higher carburization extent corresponds to higher catalytic activities in the present study, but due to the surface may be covered by wax residual or carbonous deposition, these factors will also effect the catalyst activity.

Table 4 Mössbauer spectra parameters of the catalysts after reduction[a]

Catalysts	Phases	MES parameters			Area (%)	Degree of reduction (%)[b]
		IS (mm/s)	QS (mm/s)	Hhf (kOe)		
Si0/25	Fe_3O_4 (A)	0.37	–0.07	485	2.8	48.8
	Fe_3O_4 (B)	0.68	–0.09	441	3.2	
	χ-Fe_5C_2	0.31	–0.02	219	16.6	
	ε'-$Fe_{2.2}C$	0.25	0.00	176	28.6	
	Fe^{3+}	0.35	0.85		40.0	
	Fe^{2+}	0.54	1.80		8.8	
Si5/20	χ-Fe_5C_2	0.28	0.13	216	13.9	53.2
	ε'-$Fe_{2.2}C$	0.24	0.06	174	35.5	
	Fe^{3+}	0.40	0.87		39.1	
	Fe^{2+}	0.64	2.21		11.5	
Si15/10	χ-Fe_5C_2	0.28	0.03	219	15.1	65.7
	ε'-$Fe_{2.2}C$	0.21	0.08	175	47.0	
	Fe^{3+}	0.45	0.90		27.0	
	Fe^{2+}	0.51	2.97		11.0	
Si25/0	χ-Fe_5C_2	0.30	0.07	219	19.3	59.9
	ε'-$Fe_{2.2}C$	0.21	0.07	175	37.6	
	Fe^{3+}	0.37	1.00		34.3	
	Fe^{2+}	0.54	2.97		8.7	

[a] Reduction condition: 280 °C, 0.1 MPa, H_2/CO = 1.2 and 1.0 NL/gcat/h

[b] Degree of reduction = $(A - B)/A \times 100$ where A, the mole of oxygen in the iron compounds in the fresh catalyst; B, the the mole of oxygen in the iron compounds in the reduced catalyst

3.3.2 Product Selectivity

It can be seen from Table 6, the selectivities to gaseous and light hydrocarbons (methane, C_2–C_4, and C_5–C_{11}) are suppressed, whereas those to heavy hydrocarbons (C_{12}–C_{18} and C_{19+}) are enhanced with increasing Si(P)/Si(B) ratio. But Si25/0 with only precipitated SiO_2, shows a different trend. Meanwhile, the olefin selectivities to C_2–C_4 and C_5–C_{11} for all catalysts are similar. These results may be attributed to following factors: Firstly, CO_2-TPD results

Table 5 Mössbauer parameters of the catalysts after reaction[a]

Catalysts	Phases	MES parameters			
		IS (mm/s)	QS (mm/s)	Hhf (kOe)	Area (%)
Si0/25	χ-Fe_5C_2	0.32	0.02	216	13.3
	ε'-$Fe_{2.2}C$	0.24	0.06	171	27.2
	Fe^{3+}	0.38	0.86		46.3
	Fe^{2+}	0.83	2.37		13.3
Si5/20	ε'-$Fe_{2.2}C$	0.24	0.09	168	43.8
	Fe^{3+}	0.39	0.88		41.1
	Fe^{2+}	0.90	2.22		15.1
Si15/10	χ-Fe_5C_2	0.31	0.06	216	11.8
	ε'-$Fe_{2.2}C$	0.24	0.07	170	42.9
	Fe^{3+}	0.36	0.95		35.2
	Fe^{2+}	0.63	2.01		10.2
Si25/0	χ-Fe_5C_2	0.36	–0.03	219	11.3
	ε'-$Fe_{2.2}C$	0.26	0.00	172	37.4
	Fe^{3+}	0.36	0.83		38.0
	Fe^{2+}	0.63	1.85		13.3

[a] Reaction condition: 250 °C, 1.5 MPa, H_2/CO = 0.67 and 2.0 NL/gcat/h

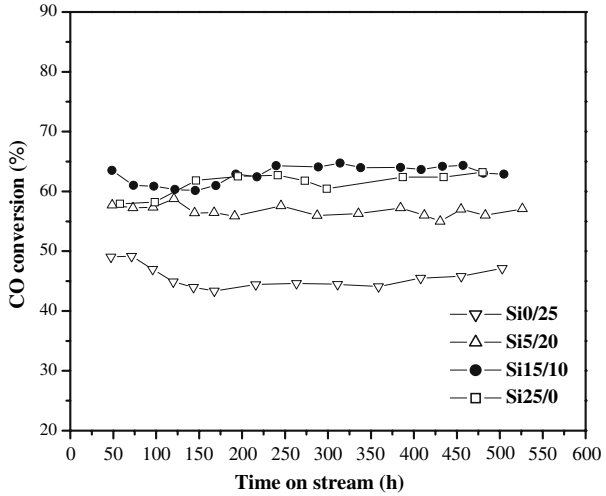

Fig. 3 The effect of Si(P)/Si(B) ratio on CO conversion. Reaction condition: 250 °C, 1.5 MPa, H_2/CO = 0.67 and 2.0 NL/g-cat/h

suggest that increasing Si(P)/Si(B) ratio improves the surface basicity of the catalyst. This would restrain the hydrogenation reaction but enhance the chain growth reaction, since the higher surface basicity of FTS iron-based catalyst can improve CO dissociative adsorption, suppress H_2 adsorption, facilitate chain growth reaction, and enhance selectivity to heavy hydrocarbons [15, 19, 30, 31]. On the other hand, partial pressure quotient, kp, which is be used as a qualitative measure of the water gas shift (WGS) reaction rate on FTS catalysts, monotonic increases with increasing Si(P)/Si(B) ratio. And the exit H_2/CO also increases with increasing Si(P)/Si(B) ratio. It implies that the catalyst with higher Si(P)/Si(B) ratio has the higher H_2/CO ratio during reaction. The higher H_2/CO ratio will enhance the hydrogenation reaction and decrease the chain growth probability [18]. The synergistic effects of the factors lead to the selectivity results.

4 Conclusions

The Si(P)/Si(B) ratio has significantly influences on physico-chemical properties of the catalysts, such as surface area, the crystallite size of the active component, the surface bacisity, reduction and carburization of the catalysts, as well as the activity and selectivity of FTS. The increase of the Si(P)/Si(B) ratio, facilitates the dispersion of the oxides (Fe, Cu, K), decreases crystallite size of iron oxide and increases the surface area, enhances the surface bacisity of the catalysts, and improves the reduction and carburization of the catalysts. However, excessive precipitated SiO_2 especially when the catalyst has only precipitated SiO_2, the effect of metal–support interaction, which suppresses the reduction and carburization of the catalysts to some extent, appears to be more pronounced.

For the FTS, with the increase of the Si(P)/Si(B) ratio, the activity increases rapidly, and passes a maximum when Si(P)/Si(B) ratio equals to 15/10 then stabilizes even declines when Si(P)/Si(B) ratio further increases. And the increase of Si(P)/Si(B) ratio, restrains the hydrogenation ability, enhances the selectivity to heavy hydrocarbons. The selectivity to light hydrocarbons increases for the catalyst with only precipitated SiO_2.

Table 6 Effect of Si(P)/Si(B) on catalyst activity and selectivity[a]

Catalysts time on stream (h)	Si0/25		Si5/20		Si15/10		Si25/0	
	311	502	384	526	314	504	387	485
CO conversion (%)	43.5	47.2	58.2	57.1	64.7	62.9	62.4	63.2
H_2 + CO conversion (%)	45.2	48.7	57.4	56.3	62.1	60.4	59.2	59.9
Exit molar H_2/CO ratio	0.63	0.63	0.71	0.71	0.81	0.79	0.82	0.83
Extent of WGS/($P_{H_2} \cdot P_{CO_2}$/Pco · P_{H_2O})	2.38	2.61	5.82	6.88	9.55	9.60	10.47	10.67
Hydrocarbon selectivities (wt.%)								
CH_4	4.8	4.8	4.2	4.1	3.7	3.7	4.5	4.6
C_{2-4}	21.5	22.2	19.7	19.6	16.3	16.0	21.3	21.6
C_{5-11}	22.6	25.5	24.0	23.1	18.5	18.1	26.9	27.1
C_{12-18}	12.7	11.8	14.1	13.0	15.5	13.3	14.7	13.3
C_{19}^{+}	38.4	35.7	38.0	40.2	46.0	49.0	32.7	33.4
Olefin selectivity (wt.%)								
C_{2-4}	82.1	81.2	81.9	81.7	82.2	81.9	82.3	82.4
C_{5-11}	81.6	82.4	80.0	80.0	82.2	81.8	82.2	81.9

[a] Reaction condition: 250 °C, 1.5 MPa, H_2/CO = 0.67 and 2.0 NL/gcat/h for 530 h

Based on the present work, a suitable Si(P)/Si(B) ratio can lead to an optimal catalytic behavior of a Fe–Cu–K–SiO_2 catalyst.

Acknowledgements We gratefully thank the financial support from the Natural Science Foundation of China (20473111), and the National Outstanding Young Scientists Foundation of China (20625620), respectively. This work is also supported by SYNFUELS CHINA.Co., Ltd.

References

1. Martínez A, López C, Márquez F, Díaz I (2003) J Catal 220:486
2. Zhang C, Yang Y, Teng B, Li T, Zheng H, Xiang H, Li Y (2006) J Catal 237:405
3. Dry ME (2001) J chem Technol Biotechnol 77:43
4. Wu B, Tian L, Bai L, Zhang Z, Xiang H, Li YW (2004) Catal Commun 5:253
5. Jothmurugesan K, Goodwin JG Jr, Gangwal SK, Spivey JJ (2000) Catal Today 58:335
6. Zhao R, Goodwin JG Jr, Jothmurugesan K, Gangwal SK, Spivey JJ (2001) Ind Eng Chem Res 40:1065
7. Sudsakorn K, Goodwin JG Jr, Jothmurugesan K, Adeyiga AA (2001) Ind Eng Chem Res 40:4778
8. Pham HN, Viergutz A, Gormley RJ, Datye AK (2000) Powder Technol 110:196
9. Bukur DB, Lang X, Mukesh D, Zimmerman WH, Rosynek MP, Li C (1990) Ind Eng Chem Res 29:1588
10. Jin Y, Datye AK (2006) J Catal 196:8
11. Wan HJ, Wu BS, Zhang CH, Xiang HW, Li YW, Xu BF, Yi F (2007) Catal Commun 8:1538
12. Zhang CH, Wan HJ, Yang Y, Xiang HW, Li YW (2006) Catal Commun 7:733
13. Dlamini H, Motjope T, Joorst G, Stege GT, Mdleleni M (2002) Catal Lett 78:201
14. Yang Y, Xiang HW, Tian L, Wang H, Zhang CH, Tao ZC, Xu YY, Zhong B, Li YW (2005) Appl Catal: Gen 284:105
15. Zhang CH, Yang Y, Teng BT, Li TZ, Zheng HY, Xiang HW, Li YW (2006) J Catal 237:405
16. Jun KW, Roh HS, Kim KS, Ryu JS, Lee KW (2004) Appl Cata A: Gen 259:221
17. Wan HJ, Wu BS, Zhang CH, Teng BT, Tao ZC, Yang Y, Zhu YL, Xiang HW, Li YW (2006) Fuel 85:1371
18. Bukur DB, Sivaraj C (2002) Appl Catal A: Gen 231 201
19. Wan HJ, Wu BS, Tao ZC, Li TZ, An X, Xiang HW, Li YW (2006) J Mol Catal A 260:255
20. Spadaro L, Arena F, Granados ML, Ojeda M, Fierro JLG, Frusteri F (2005) J Catal 234:451
21. Robert RG, Jonathan P (1987) J Catal 104:365
22. Sirmanothan N, Hamdeh HH, Zhang Y, Davis BH (2002) Catal Lett 82:181
23. Jiang M, Koizumi N, Yamada M (2000) Appl Catal A: Gen 204:49
24. Khodakov AY, Griboval-Constant A, Bechara R, Zholobenko VL (2002) J Catal 206:230
25. Guczi L, Lázár K (1991) Stud Surf Sci Catal 61:251
26. Li S, Meitzner GD, Iglesia E (2001) J Phys Chem B 105:5745
27. Li S, Krishnamoorthy S, Li A, Meitzner GD, Iglesia E (2002) J Catal 206:202
28. Sudsakorn K, Goodwin JG, Adeyiga AA (2003) J Catal 213:204
29. Mansker LD, Jin Y, Buckur DB, Datye AK (1999) Appl Catal A 186:227
30. Dry ME, Oosthuizen GJ (1968) J Catal 11:18
31. Miller DG, Moskovits M (1988) J Phys Chem 92:6081